Department of Earth Sciences, Utrecht University, The Netherlands
Department of Earth and Planetary Sciences, University of California, Santa Cruz, USA

Stable and radiogenic Sr isotope fractionation across the Paleocene-Eocene Thermal Maximum event as recorded in marine barite

Author:
Susan Pit

Supervisors:
Prof. Dr. Appy Sluijs
Prof. Dr. Adina Paytan

December 1st, 2019

Abstract

Radiogenic strontium (Sr) ratios ($^{87/86}$Sr) have historically been used to investigate weathering and hydrothermal inputs into the ocean. However, the application of $^{87/86}$Sr is limited, because it does not fractionate between seawater and Sr sinks, hence these ratios do not record the complete Sr cycle. Stable Sr ratios ($\delta^{88/86}$Sr) in seawater fractionate between seawater and carbonate, the main sink of Sr in the ocean. Therefore, $\delta^{88/86}$Sr measurements can be combined with $^{87/86}$Sr ratios to characterize the complete Sr cycle. Moreover, $\delta^{88/86}$Sr in seawater are positively correlated to carbonate burial rates. The aim of this study is to investigate $\delta^{88/86}$Sr and $^{87/86}$Sr in seawater over the Paleocene-Eocene Thermal Maximum (PETM) event using the Double Spike-Thermal Ionization Mass Spectrometry (DS-TIMS) method to investigate carbonate dissolution during the PETM. Marine barite samples from a period between 56.22-56.37 Ma were analysed. Preliminary data suggests that $\delta^{88/86}$Sr in seawater was lower (0.3‰) during the PETM than it was 75 Ma before the PETM (0.4‰). No isotopic excursion is visible in the data. Rather, seawater $\delta^{88/86}$Sr appears to reach a stable lower value during the PETM. Changes in the CCD and ocean pH at the PETM indicate that carbonate sediments have dissolved. Hence the lack of a clear signal in the $\delta^{88/86}$Sr data implies that either the excursion is not captured in the current resolution, or the seawater Sr concentrations were too high for carbonate dissolution to make a quantifiable impact. Future work to improve TIMS analysis of Sr in marine barite and increasing the temporal resolution is necessary to produce more accurate and precise data, which is necessary further explore these possible explanations.

1. Introduction

1.1. Strontium cycle

Strontium (Sr) is an alkaline earth metal often found in terrestrial mineral and marine sediments. The residence time of Sr in seawater (~2-3 Ma) greatly exceeds the mixing time of the oceans (~1 kyr) (Elderfield & Gieskes, 1982; Vollstaedt et al., 2014). Therefore, it is assumed that Sr concentrations and isotope ratios are homogeneous in the open ocean. Three Sr isotopes are considered when studying the Sr budget: stable ^{88}Sr and ^{86}Sr and radiogenic ^{87}Sr (a decay product of ^{87}Rb). Stable Sr (^{88}Sr/^{86}Sr) is reported relative to the National Institute of Standards and Technology (NIST) standard SRM987 according to the following equation:

$$\delta^{\frac{88}{86}}Sr(‰) = \left(\frac{\frac{88Sr}{86Sr_{sample}}}{\frac{88Sr}{86Sr_{SRM987}}} - 1 \right) * 1000$$

The accepted ^{88}Sr/^{86}Sr value of SRM987 is 8.37515 (Böhm et al., 2012). Radiogenic strontium(^{87}Sr/^{86}Sr) is reported as an absolute isotope ratio.

The Sr budget of the global ocean is governed primarily by inputs of fluvial discharge, hydrothermal activity, and groundwater discharge (Fig.1). The primary sink for Sr in seawater is calcium carbonate ($CaCO_3$) deposition. Sr substitutes for calcium in the calcium carbonate lattice, and ^{86}Sr is incorporated preferentially over ^{88}Sr. This fractionation results in an average $\delta^{88/86}$Sr of ~0.15‰ for modern carbonates. Modern seawater $\delta^{88/86}$Sr is 0.39‰ (Vollstaedt et al., 2014; Pearce et al., 2015). The sources and sinks in the Sr cycle have different isotopic

compositions. Therefore, changes in the isotopic composition of Sr in seawater indicate changes in the relative contribution and composition of fluxes in the Sr cycle.

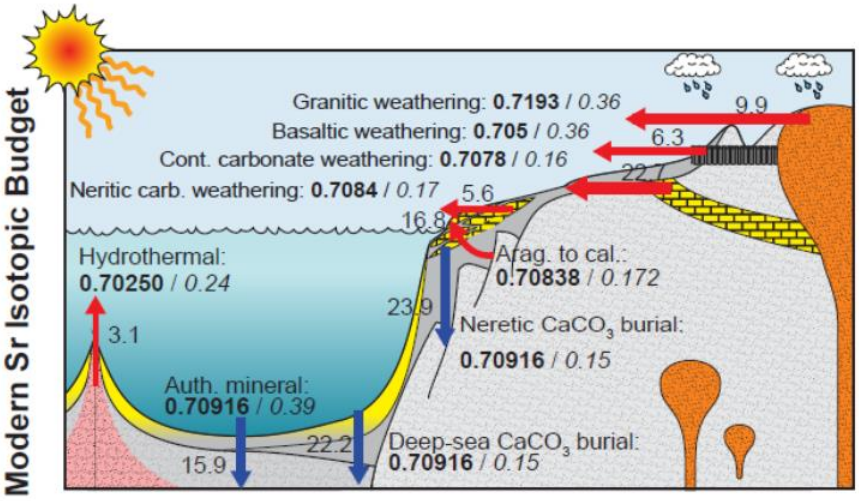

Figure 1: A schematic depiction of the modern Sr cycle. Bold numbers indicate mean radiogenic Sr ratios, italic numbers indicate mean stable Sr ratios, normal numbers indicate fluxes in Gmol yr^{-1}. (Paytan et al., submitted).

Radiogenic Sr isotopic ratios ($^{87}Sr/^{86}Sr$) in the ocean are commonly used to study the relative inputs of Sr from weathering sources, tectonic activity, and hydrothermal inputs (Frank, 2002; Vollstaedt et al., 2014). $^{87}Sr/^{86}Sr$ has steadily increased over the past approximately 40 Ma, with a variable rate of change over time (Hess et al., 1986; Palmer & Elderfield, 1985). This increase is thought to be primarily due to changes in silicate rock weathering and consequently the fluvial runoff into the ocean, but the weathering flux is not completely constrained (Allègre et al., 2010; Mokadem et al., 2015; Palmer & Elderfield, 1985). Changes in the isotopic signature of the weathering rocks may also explain the observed trend.

Stable strontium ($^{88}Sr/^{86}Sr$) in sea water is influenced primarily by $CaCO_3$ sequestration in marine sediments (Vollstaedt et al., 2014). The sequestration flux of $CaCO_3$ to deep-sea sediments is important to quantify, as it is the main sink of carbon in the long-term global carbon cycle. Deep-sea sediments are a large, long-term reservoir in the global carbon cycle, where carbon is stored in the form of carbonate. It is likely that perturbations in atmospheric carbon dioxide (CO_2), such as during the Paleocene Eocene Thermal Maximum (PETM), will correspond to changes in carbonate burial or dissolution because of ocean acidification caused by atmospheric CO_2 equilibration with seawater (Emerson & Hedges, 2008). Neretic (shelf) carbonates incorporate relatively more Sr per mass of carbonate than pelagic (deep) carbonates (Stoll & Schrag, 1998). The stable Sr isotopic composition of the ocean is therefore more strongly affected by neretic carbonate deposition/dissolution changes than by pelagic carbonate deposition changes.

Recent studies have demonstrated the use of paired radiogenic and stable Sr isotopes as a tool for constraining both weathering and carbonate deposition fluxes to study the Sr budget in the modern ocean (Allègre et al., 2010; A. Krabbenhöft et al., 2010; Pearce et al., 2015; Vance et al., 2009).This method will be applied to study the oceans and global carbon cycle during the PETM.

The Sr isotope ratios provide constraints on changes in both the magnitude and composition of fluxes. Measuring and quantifying $^{87}Sr/^{86}Sr$ in seawater is important to better

understand the total weathering input into the global oceans. Measurements of $\delta^{88/86}Sr$ also contribute to better understanding weathering fluxes, which affect the alkalinity of the ocean and influence carbonate deposition. Carbonate deposition can be inferred based on $\delta^{88/86}Sr$ (Krabbenhöft et al., 2009). Analysing $\delta^{88/86}Sr$ in tandem with $^{87}Sr/^{86}Sr$ will allow for a more detailed analysis of the fluxes in the Sr cycle. Here, I use paired stable and radiogenic Sr isotope records to study a period further back in time, when abrupt climate change may have changed the relative balance of the input and output fluxes of Sr to the ocean.

This study aims to reconstruct stable ($\delta^{88/86}Sr$) and radiogenic ($^{87}Sr/^{86}Sr$) Sr isotope ratios of seawater using marine barite over the PETM. The PETM is of interest because of the shoaling of the carbonate compensation depth (CCD) and associated carbonate dissolution observed in the geological record. This carbonate dissolution is expected to be reflected by decreased stable Sr isotope ratios due to release of ^{86}Sr into seawater when carbonate dissolves. Reported here are the results of method development for measurements of Sr isotopes in marine barite and preliminary data over the PETM.

1.2. The Paleocene-Eocene Thermal Maximum

The PETM was a climatic perturbation event around ±56 Ma that lasted approx. 170kyr during which global temperatures and atmospheric CO_2 increased rapidly (McInerney & Wing, 2011; Penman et al., 2014; Röhl et al., 2007; Zachos et al., 2005). It is of particular interest to scientists as a parallel to current climate change, though not a perfect analogue. The global carbon cycle changed during the PETM because of the addition of massive amounts of carbon to the atmosphere, much like today's carbon cycle is affected by anthropogenic emissions. During the PETM, atmospheric carbon equilibrated with the global oceans and caused acidification (Zachos et al., 2005). Deep sea sediments deposited during the PETM are characterised by abnormally low $CaCO_3$ content (<1 wt%) due to massive carbonate dissolution (Zachos et al., 2005).

Since $\delta^{88/86}Sr$ of seawater is sensitive to carbonate burial and dissolution, a $\delta^{88/86}Sr$ excursion associated with the massive oceanic carbonate dissolution is expected. An estimate of the excursion in the stable strontium ratio through the PETM can be made based on an approximation of the carbonate dissolution Estimates of the amount of carbon (C) released into the atmosphere lie between 3000 and 9000 pG C (McInerney & Wing, 2011; Ridgwell, 2007). To make an estimate of how this carbon input and subsequent carbonate dissolution affected the $\delta^{88/86}Sr$ of seawater, the assumption is made that effectively all of this carbon was dissolved into the ocean and neutralised through the carbonate (CO_3) buffer system, where for each mole of dissolved atmospheric carbon, one mole of carbonate is released from the sediments through dissolution (Fig. 2; Eq. 2). Accordingly, the following calculations should provide a numerical estimate of the maximum (Eq. 1a) and minimum (Eq. 1b) amount dissolved:

$$g\ C\ in\ atmosphere * MolWeight\ carbon = mol\ C\ absorbed\ in\ ocean \quad (1)$$

$$3e18 \cdot 12.01 = 2.5e17 \quad (1a)$$

$$9e18 \cdot 12.01 = 7.5e17 \quad (1b)$$

$$mol\ C\ absorbed\ in\ ocean = mol\ CO_3\ dissolved\ from\ sediments \quad (2)$$

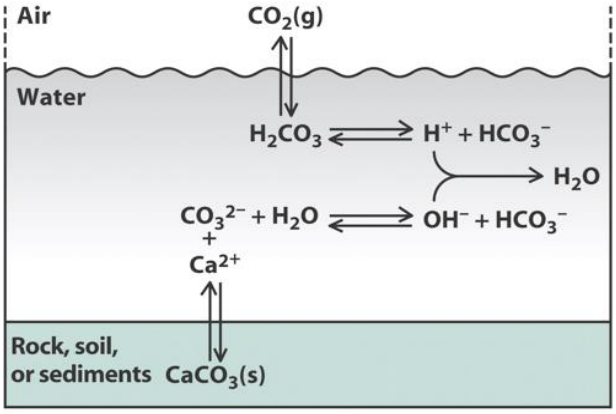

Figure 2: The carbonate buffer mechanism involved in carbon dioxide dissolution in the ocean (Cuker & Bugyi, 2016).

There are two potential endmember situations associated with carbonate dissolution. The first is that all of the carbonate that dissolved was shelf carbonate. The second endmember is that all of the carbonate that dissolved was deep carbonate. The only difference between these two endmembers is the partitioning coefficient of Sr. The two partitioning coefficients of Sr into carbonate are 0.176 for deep carbonates and 0.9 for shelf carbonates (Stoll & Schrag, 1998). These partitioning coefficients are multiplied with the number of moles of carbonate that dissolve, forming 4 different situations: 3000 Pg carbon released with deep carbonate dissolution (3d), 3000 Pg carbon released with shelf carbonate dissolution (3s), 9000 Pg carbon released with deep carbonate dissolution (9d), and 9000 Pg carbon released with shelf carbonate dissolution (9s). This amounts to four different estimates for the amount of Sr released during carbonate dissolution (Table 1).

Table 1: Four endmember estimates of the amount of Sr released into seawater through carbonate dissolution and subsequent $\delta^{88/86}$Sr of seawater.

Moles of Sr released into seawater		
Amount of carbon dissolved into seawater	**Carbonate dissolution partitioning**	
	Only deep carbonate	**Only shelf carbonate**
3000 Pg	$4.4 \cdot 10^{16}$ moles (3d)	$2.25 \cdot 10^{17}$ moles (3s)
9000 Pg	$1.32 \cdot 10^{17}$moles (9d)	$6.74 \cdot 10^{17}$ moles (9s)
$\delta^{88/86}$Sr of seawater after carbonate dissolution		
3d	0.33‰	
3s	0.24‰	
9d	0.27‰	
9s	0.19‰	

The concentration of Sr in seawater just before the PETM is unknown, but it is assumed that it is around 87uM based on modern seawater concentrations (Stoll & Schrag, 1998). Using an estimate of the global ocean volume ($1.4 \cdot 10^{21}$ L) the number of moles of Sr in the ocean is calculated to be $1.22 \cdot 10^{17}$ moles. The $\delta^{88/86}$Sr of seawater just prior to the PETM is close to that of modern seawater at approximately 0.4‰ (Vollstaedt et al., 2014). The $\delta^{88/86}$Sr of carbonate is the same for shelf and deep carbonates: 0.15‰ (Pearce et al., 2015).

$$\delta^{88/86}Sr_{sw\ after\ dissolution} = \frac{mol\ Sr_{sw} \cdot \frac{\delta 88Sr}{86Sr}_{sw} + mol\ Sr_{carb} \cdot \frac{\delta 88Sr}{86Sr}_{carb}}{mol\ Sr_{sw} + mol\ Sr_{carb}} \quad (3)$$

Equation 3 gives different estimates for the $\delta^{88/86}$Sr in seawater after carbonate dissolution for each endmember (Table 1). Those values correspond to negative excursions between -0.07‰ and -0.21‰. The $\delta^{88/86}$Sr of seawater in the Phanerozoic has been found to be between ~0.25‰ and ~0.60‰ (Vollstaedt et al., 2014). The PETM seawater $\delta^{88/86}$Sr estimates (Table 1) fall mostly within this range, indicating that these are reasonable estimates.

The most likely cause of carbonate dissolution in the PETM was the shoaling of the CCD by over 2 km to <1 km (Zachos et al., 2005; Zeebe et al., 2009). It is an adequate assumption that this mostly affected pelagic carbonate deposition/dissolution fluxes, because a shoaling CCD would most prominently affect the basin environment, and might not even reach the shelf environment (±150 m) in places. Shoaling of the CCD would cause mass dissolution of pelagic carbonates before it would initiate dissolution of neretic carbonates. Hence endmembers 3d and 9d are probably closer to reality, with excursions between -0.07‰ and -0.13‰.

A sensitivity analysis can be done to test the robustness of the assumptions made to procure this estimate of the Sr stable isotope excursion. The initial assumption concerns the amount of carbon released into the atmosphere, and how much of this equilibrates with the ocean. Varying this value indicates that inaccurate estimates of this value have an effect on the final estimated stable Sr ratio in seawater (Fig. 3). Higher estimated amounts of carbon equilibrating with seawater leads to more strongly negative stable Sr isotope ratios. In the range that is considered for the PETM (3000-9000 Pg) this variation seems approximately linear with a gradual slope for both shelf and deep dissolution, indicating that rough estimates are reasonably robust. In the range of smaller amounts of carbon equilibrating with seawater, the slope is steeper and for neretic carbonate dissolution it becomes less linear.

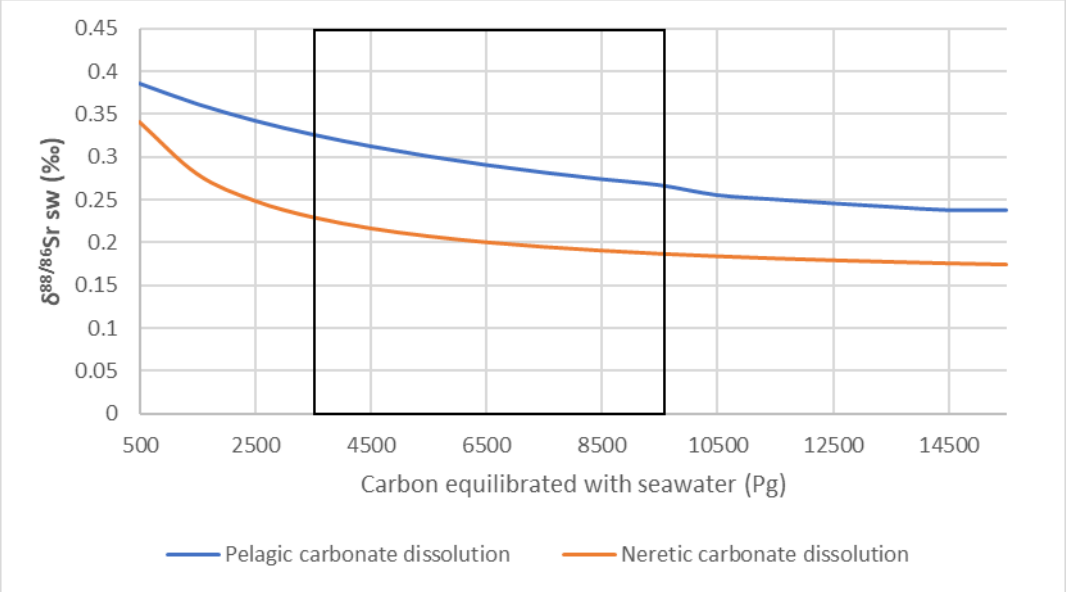

Figure 3: Sensitivity of $\delta^{88/86}$Sr in seawater to the estimated amount of carbonate released into the atmosphere. The black square indicates the range of amounts assumed in our calculations: 3000-9000 Pg carbon.

Another assumption concerns the $\delta^{88/86}Sr$ in carbonates. Reported modern values range between 0.15‰ and 0.21‰ (Krabbenhöft et al., 2010; Pearce et al., 2015). Higher estimates of $\delta^{88/86}Sr$ in carbonates yield more conservative estimates of the $\delta^{88/86}Sr$ in seawater, as it is closer to the initial stable Sr ratio in seawater (~0.4‰) (Fig. 4). The assumed $\delta^{88/86}Sr$ in carbonate is linearly related to the final $\delta^{88/86}Sr$ in seawater. Estimating this value is difficult, as carbonates record the $\delta^{88/86}Sr$ in seawater (with a fractionation factor of -0.24‰) and are thusly correlated to $\delta^{88/86}Sr$ in seawater when the carbonates were formed, which is unknown (Krabbenhöft et al., 2010; Vollstaedt et al., 2014).

The $\delta^{88/86}Sr$ of seawater between 125 Ma and the PETM at 56.3 Ma is unknown, so nothing definitive can be said about the $\delta^{88/86}Sr$ of carbonates formed in that period. About 160 Ma the $\delta^{88/86}Sr$ of seawater was close to 0.30‰, after which it gradually increased to approximately 0.40‰ at 140Ma (Vollstaedt et al., 2014). It remained relatively stable between 140 Ma and 125 Ma. This means that carbonates that formed between 160 Ma and 140 Ma have a lower $\delta^{88/86}Sr$ than carbonates formed between 140 Ma and 125 Ma. Much like in modern seawater, between 160 Ma and 125 Ma the $\delta^{88/86}Sr$ of seawater was always lower than 0.4‰, indicating that perhaps modern or lower estimates for $\delta^{88/86}Sr$ of carbonates could be accurate even if it yields less conservative results (Vollstaedt et al., 2014). However, it is difficult to estimate when the carbonates that dissolved during the PETM were formed, so this is mostly speculation.

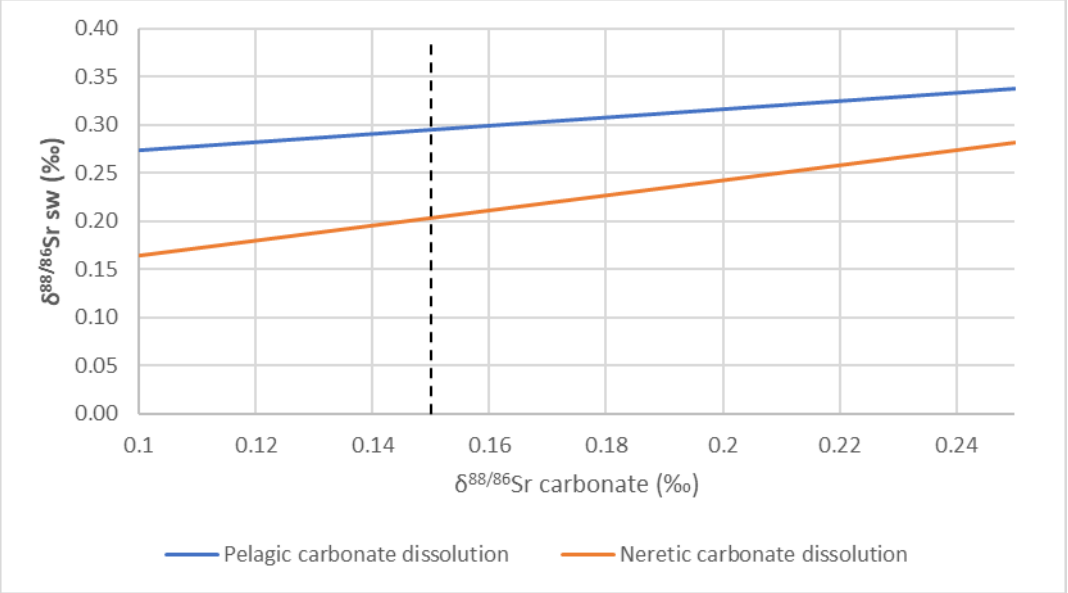

Figure 4: Sensitivity of $\delta^{88/86}Sr$ in seawater to the estimates of $\delta^{88/86}Sr$ of carbonates when 6000 Pg carbon is released into the atmosphere. The black arrow indicates the assumed value for our calculations (0.15‰).

The last assumption to be considered is the initial concentration of Sr in seawater. The sensitivity of the calculation to this parameter largely depends on the assumed Sr input from carbonate dissolution, as that balances out the Sr already in seawater. With low initial seawater Sr concentrations, $\delta^{88/86}Sr$ in seawater shifts to a composition purely caused by carbonate dissolution; 0.15‰ (Fig. 5). With high initial seawater Sr concentrations, $\delta^{88/86}Sr$ in seawater shifts to a situation where carbonate dissolution has no significant effect and it remains at the initial ratio of 0.4‰. Presently there is no record to constrain the Sr concentration to reduce this uncertainty..

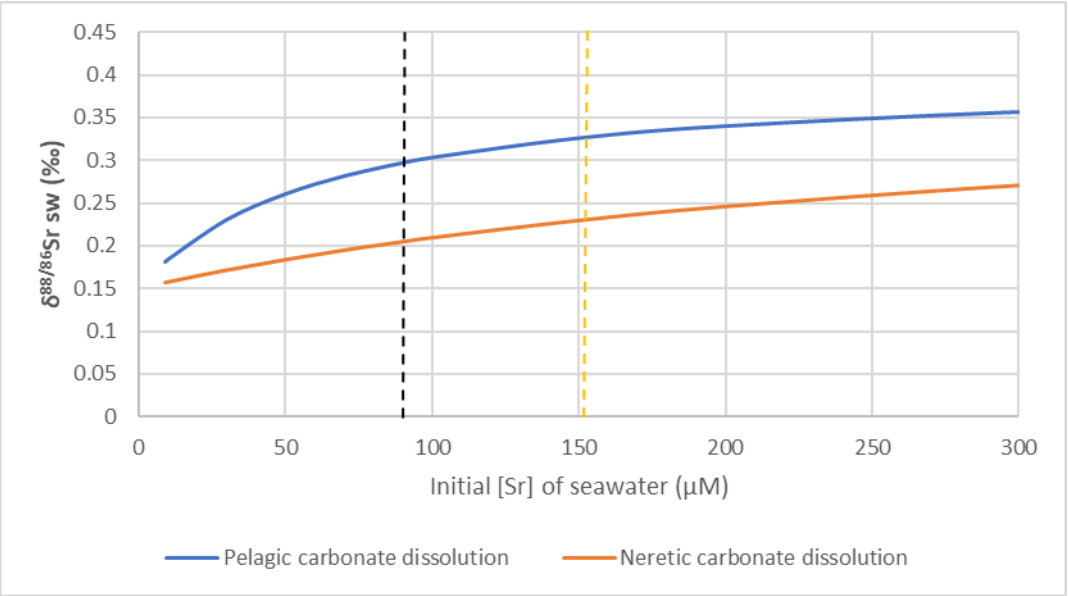

Figure 5: Sensitivity of $\delta^{88/86}Sr$ in seawater to the estimated initial Sr concentration in seawater when 6000 Pg carbon is released into the atmosphere. The black line indicates the concentration assumed in the calculation (87 µM). The orange line indicates a modeled value estimated by Vollstaedt et al., (2014).

1.3. Strontium in barite

$CaCO_3$, as an important sink for Sr, is often used as a to create a past Sr isotopic record of seawater. During the PETM, carbonate was massively dissolved in deep sediments and therefore is only available in shallow sediment cores. These shallow carbonates are likely affected by diagenesis, which alters the isotopic signature they record. Thus, the carbonate record for the PETM is sparse and unreliable, and another archive must be used to reconstruct seawater Sr isotopes.

In sediments where $CaCO_3$ is diagenetically altered or unavailable, barite is a reliable alternative for the reconstruction of Sr isotopic records (Mearon et al., 2003). Marine barite is a good alternative for carbonate when recreating Sr records, as Sr replaces Barium (Ba) in the crystal lattice (Paytan et al., 1993). Marine barite precipitates directly from seawater in microenvironments and thus records seawater chemistry. Further, marine barite is resistant to diagenesis and dissolution (Mearon et al., 2003; Paytan et al., 2002). Barite can also precipitate in other environments (e.g. hydrothermal systems), so care must be taken to identify pristine marine barite based on crystal size, crystal morphology, and isotopic composition for palaeoceanographic studies (Paytan et al., 2002). Using barite not only solves the issue of low carbonate availability in PETM sediments, it also does not share carbonate's sensitivity to diagenesis and dissolution nor the temperature and vital effects that impact Sr incorporation into biogenic carbonates. Overall, barite is a more reliable and continually available archive for PETM Sr isotopes.

1.4. Current limitations and the DS-TIMS

When using traditional methods, the $^{87}Sr/^{86}Sr$ ratio is normalised to the fixed $^{88}Sr/^{86}Sr$ ratio to correct for mass dependent isotope fractionation, so the value of $^{88}Sr/^{86}Sr$ cannot be determined (A. Krabbenhöft et al., 2010). This can also be overcome by applying the Thermal

Ionization Mass Spectrometry Double Spike (DS-TIMS) method, allowing $^{88}Sr/^{86}Sr$ to be studied as well as $^{87}Sr/^{86}Sr$ (Krabbenhöft et al., 2009). The DS-TIMS method removes the necessity to normalize the $^{87}Sr/^{86}Sr$ ratio of a sample to a fixed $^{88}Sr/^{86}Sr$ ratio to correct for mass dependent isotope fractionation by measuring the sample twice: once spiked with Sr with a known isotope ratio and once unspiked (Krabbenhöft et al., 2009). Thus each sample involves two measurements. The true ratios are assumed to be related to the measured ratios through an exponential function involving the masses of the isotopes and a specific fractionation factor for each sample, spiked and unspiked (Krabbenhöft et al., 2010). The sample to spike ratio is known, and the isotopic composition of the spike is known. The fractionation factors are the unknowns that are calculated by making an initial estimate with a linear function, followed by a series of iterations. The final value has an error margin that can be minimized by calibrating your sample:spike ratio. The ratio utilized in this study was ~4:1, providing an error margin of ~0.000005.

Past studies have successfully extracted a Sr fraction from barite through column chromatography (Paytan et al., 1993; Paytan et al., 2002). Isotopes can fractionate during the column chromatography procedure, because a cation exchange resin separates based on mass and isotopes have minute mass differences (Teng, 2017). A reproduction of Paytan et al.'s column chromatography method resulted in a ~97% yield in this study. This yield is sufficient for double spike method measurements, as this method accounts for fractionation on the TIMS as well as on the column.

2. Methods

2.1. Sample selection

Samples within the PETM were selected, and come from a single core (Table 2). More samples will be processed in the future with the goal of covering the entire PETM in a single core and having samples from other cores to confirm that any observation is not local. This core was collected on leg 199 of the Ocean Drilling Project, and is located in the Equatorial Pacific (Fig. 6).

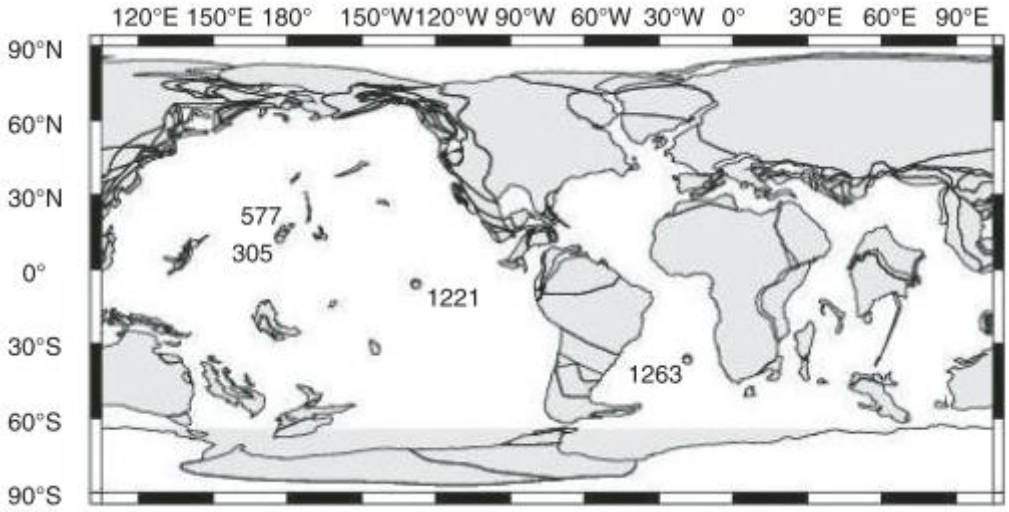

Figure 6: Location of the sampling site (1221) (Paytan et al., 2007).

Table 2: Sample selection.

Site	Section	Depth (cm)	Age (ma)[a]
1221C	11-3	54-56	56.252
1221C	11-3	110-113	56.3276
1221C	11-3	140-142	56.3691
1221C	11-3	98-100	56.3111
1221C	11-3	94-96	56.3055
1221C	11-3	90-92	56.3000
1221C	11-3	80-82	56.2611
1221C	11-3	45-48	56.2232
1221C	11cc	9-12	56.3458
1221C	11-3	70-72	56.2724
1221C	11-3	84-86	56.2917

[a]Yao et al., 2018

2.2. Barite separation from sediments and dissolution

Barite was separated from deep sea sediment samples in a series of leaching steps (Table 3) (Paytan et al., 1993). In between the steps, the sediment was rinsed thoroughly with Milli-Q water (MQ) and separated through centrifuging.

Table 3: Steps involved in leaching barite from bulk sediments (Paytan et al., 1993).

Steps	*Description*
1	HCl was added to crushed, dried sediment to remove carbonates.
2	Bleach was added and let to react overnight in a 50°C oven to remove organic materials.
3	Hydroxylamine in acetic acid is added to remove transition metals.
4	HF and nitric acid is added and left to react overnight to remove silicates. Depending on the amount of silicates in the sample, repeat.
5	AlCl and nitric acid is added to remove fluorides, and left to react overnight in a 80°C oven.
6	The sample is ashed in a 700°C furnace to remove organic residue.
7	(Optional) Check sample for purity with XRD.

Following the leaching procedure, the barite was dissolved using a cation exchange resin in excess that bound the cations and left the anions in solution (Table 4).

Table 4: Steps involved in dissolving barite.

Steps	*Description*
1	Place the desired amount of solid barite in a Teflon beaker and add approx. 1mL cation exchange resin.
2	Fill beaker with MQ water.
3	Place in 90 degree Celsius oven overnight.
4	If pH in beaker is lower than approx. 4, decant the liquid into a bottle to collect dissolved anions, and add new MQ to Teflon beaker.
5	Repeat step 4 until pH no longer decreases and there is no visible solid barite anymore.
6	If there is still visible solid barite, add more resin and repeat the steps above this one.
7	If the pH is no longer decreasing and there is no visible solid barite anymore, put the resin from the Teflon beakers into a column and run 8N HCl and 2N HNO_3 over the columns to elute all the cations from the resin.
8	Collect column elution containing all cations in a beaker, and collect leftover resin in another beaker.

2.3. Strontium elution from barite

After the dissolution of solid barite, Sr is still dissolved with other cations such as barium, calcium and magnesium. Concentrations were measured using the Thermo Scientific Element XR. The separation of Sr from those other cations is achieved through column chemistry using a cation exchange resin. This resin separates elements on the basis of mass. The resin used was Bio-Rad AG-50W-X8 (AG50), The dry mesh size of AG-50 resin inversely affects the flow rate, so for the extremely narrow columns used in this instance a smaller dry mesh size was used to allow for more pore space in the wet resin. Thus the calibration of this procedure is adapted to the column dimensions of our specific columns and AG50 resin dry mesh size (Table 5).

Table 5: Steps involved in column separation of cations .

Steps	*Description*
1	Clean columns thoroughly with 6N HCl and follow with a MQ rinse.
2	Fill columns with 1.8N HCl, make sure there are no bubbles.
3	Load resin up to the bottom of the reservoir in the 1.8N HCl, allow to settle. [a]
4	Pipette excess 1.8N HCl off.
5	Condition resin with 2mL 1.8N HCl.
6	Load sample in 100uL 0.75N HCl.
7	Run through 5mL 1.8N HCl and collect in a teflon, this contains most of the lighter cations such as calcium.
8	Run through 1 mL 1.8N HCl and collect, this is the first safety fraction.
9	Run through 4mL 1.8N HCl and collect, this is the Sr fraction.
10	Run through 2 mL 1.8N HCl and collect, this is the second safety fraction and provides a buffer between the Sr and the Ba.
11	Run through 5mL 6N HCl and collect, this contains Ba and rare earth elements.

[a]: Due to slight differences in the volumes of the used columns, this means some columns have more resin than others. This did not produce significantly different elution curves between columns.

This method has a yield of approximately 97%, with Ba and Mg completely separated from Sr (Fig. 7). Mg elutes in the first 3 mL of 1.8N HCl. Sr elutes in 6-10mL 1.8 HCl. Ba elutes completely in the last 5 mL of 6N HCl. Ca elutes somewhat unsteadily in the first 8-9mL, causing some Ca to be present in the Sr fraction. This did not appear to affect TIMS measurements, as the samples still ionized well in the TIMS.

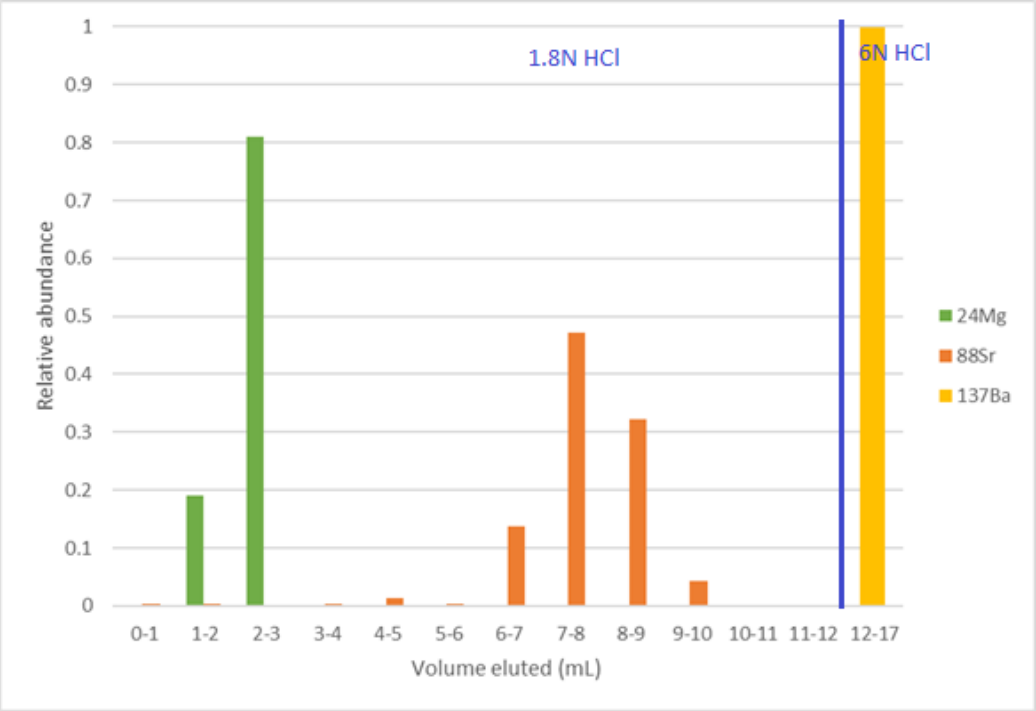

Figure 7: Elution curve of Mg, Sr, and Ba. 0-12 mL is 1.8N HCl, 12-17 mL is 6N HCl.

Prior to use, the resin was cleaned on columns using 6N HCl. This step was implemented after discovering that bulk cleaning the resin was not sufficient and resulted in

a high column blank. To assess whether this affected the quality of samples run previously, blank columns were run with the unclean resin. The purpose of these blanks was to investigate whether the contamination would affect the Sr fraction significantly. This was found to not be the case (Fig. 8). Strontium from barite samples elutes in 6-10mL, so it is crucial that this fraction is not affected by contamination. Neither Sr nor Ba from resin contamination eluted in that fraction, implying that Sr samples run over bulk-cleaned resin were likely not significantly affected. Nonetheless, resin was cleaned both in bulk and over columns for the remainder of the project.

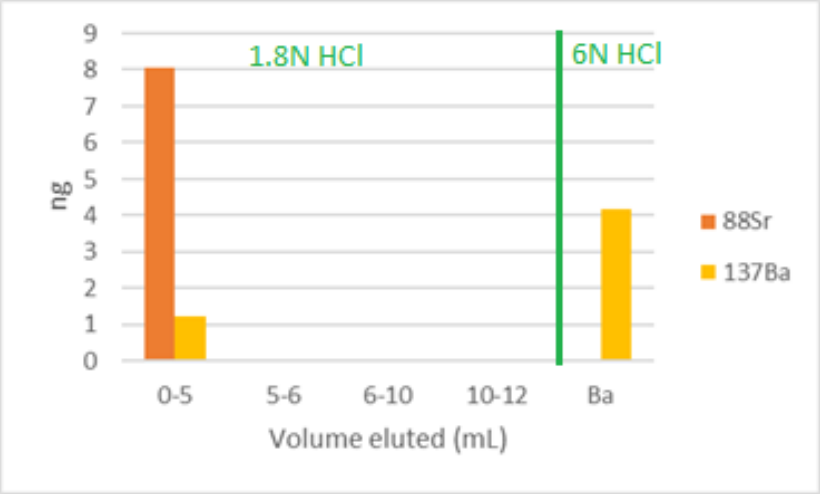

Figure 8: A blank AG50 column run with unclean resin. The 6-10 mL fraction is the fraction where Sr from barite samples elutes. There is no measurable quantity of Sr or Ba eluting between 6-10 mL.

2.4 Comparing column chemistry methods

Other potential methods for Sr separation from barite were considered before the abovementioned method was chosen. Scher et al. (2014) published a method using Sr-spec, where using less resin was found to produce a Sr fraction with little Ba in it. Attempts at reproducing this method were unsuccessful. Problems such as too much Ba in the Sr fraction, or Sr elution being too spread out could not be solved.

AG50 and Sr-Spec can both be used to separate Sr from minerals through column chemistry but do so in different ways. Therefore, these different resins should be calibrated and the procedures to use them are resin specific.

AG50 is a cation exchange resin and separates Sr by separating each element based on mass and charge. Lighter elements elute first, heavier elements last. For barite this means that Mg will elute first, followed by Ca, Sr, Ba and other rare earth elements. Higher normality acids release cations from the resin faster than lower normality acids. Hence, for a greater separation of the cations a lower normality acid should be used. This requires more acid volume to pass over the resin to elute the cations and thus separating the cations from each other takes a considerable amount of time. To increase the efficiency of the procedure it is important to balance acid use, which increases the blank, and the time it takes to achieve the separation. As a final step high normality acid is run over the column to elute all the cations left in the resin. This can also be considered as a cleaning step to make sure the sample is completely eluted and no cations (other than H^+) remain on the resin. The calibration of cation

exchange resins is straightforward: if elements are not well separated, use lower normality acid.

Sr Spec is a stick/non-stick resin that only binds Sr. Other elements do not bind to the resin and run directly through the column. High normality acids do not release Sr from the resin, while low normality acids do. Calibrations of Sr Spec for this project were attempted using low normality (0.05N) HNO_3 to elute Sr. The initial step to remove all elements except Sr from the resin is to elute with high normality acids. After all other elements are removed, low normality acid is run over the column to release Sr from the resin. Cleaning this resin is done on the column through a series of alternating steps of MQ water and high normality acid. The calibration of this Sr-Spec column is simple in theory: run enough high normality resin to remove anything but Sr and then elute Sr with as much low normality acid as necessary. In practice this is more complicated when trying to separate Sr from barite. Sr-Spec tends to display history effects, where Ba elutes a little bit all throughout the elution curve. Strontium also sometimes does not bind to the resin completely and elutes with high normality acids (Fig. 9). Other studies have had similar issues, but eventually developed a working method (Ohno & Hirata, 2007; Scher et al., 2014). Their methods could not be reproduced to be used in this study because Ba did not elute consistently in the same fraction and tailed off into the Sr fraction too much. This is likely due to small differences in the column geometries used between studies.

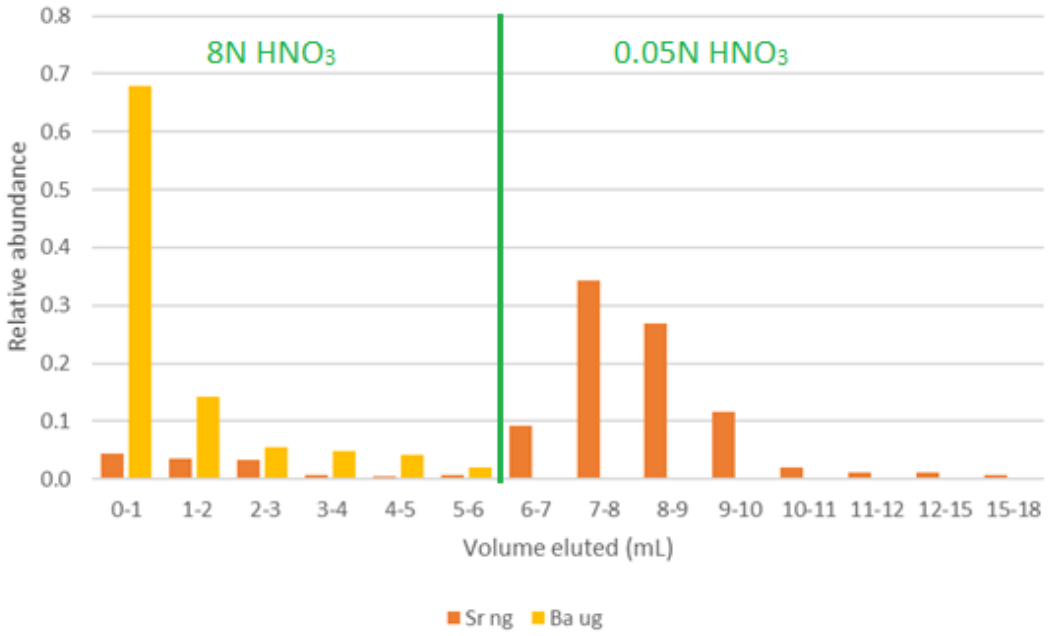

Figure 9: Sr from the sample in this case elutes slightly in 0-6 mL, which is 8N HNO_3 and should not elute Sr from the resin. The resin capacity was not exceeded. The reason that Sr elutes in high normality acid here is unknown.

2.5. Strontium isotopic fractionation measurements

Strontium, isolated from marine barite samples by column chromatography, was analysed in the TIMS for its isotope ratios. Samples were cleaned with concentrated nitric acid and hydrogen peroxide and dried down with a drop of low normality phosphoric acid. The latter makes the sample dry down to a single drop with a gel-like texture, which makes it easier to find the sample in the beaker and collect it completely to load it on the filaments. Rhenium,

non-zone refined filaments were used. The sample is loaded using a TaCl activator, with ideal loads being below 300ng Sr. After loading, each sample is smoked: a voltage is run through the filament until it burns red hot after which the voltage is quickly reduced to zero. SRM987 was used as an internal standard, while JCP and NASS-6 were used as external standards.

This project was an initial attempt at analysing Sr isotopes in barite using the TIMS double spike. As such, the results are subject to large uncertainties and a large part of this project was focused on refining the loading and running procedures. The preliminary methods and variations discussed are subject change in future work.

The $^{86}Sr/^{88}Sr$ ratio throughout the measurement can be diagnostic of good versus poor runs (Fig. 10). This ratio should decrease evenly as the sample fractionates. Sharp breaks or jumps in the trend are thought to indicate reservoir effects on the filament. Reservoir effects can occur when distinct pools of the sample are ionized from the filament at different times during the run. For example, a decreasing 86/88 ratio trend may suddenly jump to higher 86/88 ratios before continuing to decrease (Fig. 10, upper panel) indicating the first pool of sample on the filament was exhausted and the second pool began fractionating. The use of parafilm "dams" on the filaments was attempted to minimize reservoir effects, but did not appear to improve the fractionation of the samples.

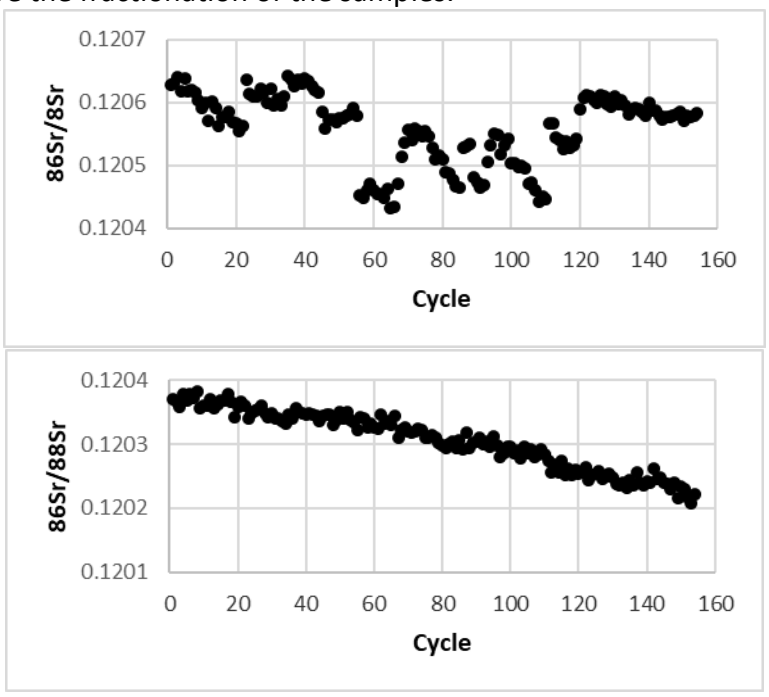

Figure 10: $^{86}Sr/^{88}Sr$ ratios in samples over the complete 160 cycles of each TIMS run. The upper panel shows a sample that did not run well because of reservoir effects and should not be used (1221C 11-3 140-142), the lower panel shows a sample that ran well and can be used (1221C 11-3 80-82).

Further improvements to the TIMS measurement procedure were made based on the recommendations of other research groups doing similar analyses. The current procedure is described here.

Each sample is ramped to a temperature of approximately 1350 degrees Celsius and allowed to stabilize while contaminants burn off and the source vacuum is below $5e^{-8}$ mbar. This reduces background noise in measurements. When the vacuum is below this threshold, the line of sight is opened and the each sample is tuned individually to have better control over the measurement. The tuning procedure starts with making sure the peaks of all faraday

cups are aligned to make sure none of the measurements are made on the side of peaks where larger variabilities occur due to small peak shifts during the measurement. Afterwards, other parameters, such as the lens position and sample extraction volume per time, are tuned to maximise intensity and stability. This is done by going over all the parameters manually once, running an autotune, and then going over all the parameters manually again. Then the sample is left to sit until all the Rubidium has burned off. Subsequently, the sample is ramped until the signal of ^{88}Sr over the axial cup has reached 2 volts and is allowed to stabilize for 10 minutes. Our samples usually gradually increase during this step, or they remain stable. After 10 minutes at 2 volts, the ^{88}Sr signal is ramped up to 5 volts and the measurement is initiated. . Each measurement includes 15 blocks of 11 cycles with a background noise measurement done between each block.

Clear parameters for quality control are currently in the process of being established. Current and future work is focused on investigating what measured values could be parameterized to qualify good or bad samples. These include but are not limited to measuring a large number of standards, observing how accurate and precise the measurements are, and linking this to patterns in measured values such as ^{88}Sr/^{86}Sr or intensity. The data reported here were assessed through a preliminary set of criteria, where sample fractionation patterns were primarily used to distinguish between “good” and “bad” runs.

The raw data from the TIMS software was run through a program written by Neymark et al. (2014), which calculates the isotope ratios in the samples using the double spike data reduction algorithm. The data reduction program allows for the exclusion of cycles that displayed reservoir effects during the run. In this way, the impact of these reservoir effects on the results was minimised, though this should still be considered a large source of uncertainty in the current method. The stable Sr isotope ratio is internally corrected against SRM987 measurements with an offset:

$$Offset = \left(\frac{\frac{88Sr}{86Sr}measured}{\frac{88Sr}{86Sr}literature} - 1\right) * 1000$$

This offset was subtracted from the sample measurements. The radiogenic Sr ratio was corrected against a known value of 0.71024 (Krabbenhöft et al., 2009):

$$\frac{\frac{87Sr}{86Sr}measured}{0.71024} = correction\ factor$$

Each radiogenic Sr ratio was corrected by multiplying it with this correction factor, and each turret has its own correction factor.

3. Results

3.1 Element ratios

Barite incorporates a series of trace elements into its lattice, and can therefore be an indicator of seawater concentrations of those cations (Paytan et al., 1993). It incorporates several elements of interest, such as Ca and Mg. Barite samples for this study were dissolved using ion exchange resin, which does not dissolve 100% of the barite sample and dissolves

ions incongruently making it inaccurate for element ratio analyses (Averyt et al., 2003). Hence these ratios should be considered as an indication more so than an absolute truth. Sr/Ba varies around 0.024, Ca/Ba varies around 0.014, Mg/Ba varies around 0.0075 and all three are relatively stable over the PETM (Fig. 11). Sr/Ba remains stable until approximately 15 kyr after the PETM onset when it increases until 30 kyrs after the onset of the PETM, after which it returns to the initial ratio. Ca/Ba and Mg/Ba do not have definitive trends over the period covered by the data, and Mg/Ba data experiences scatter.

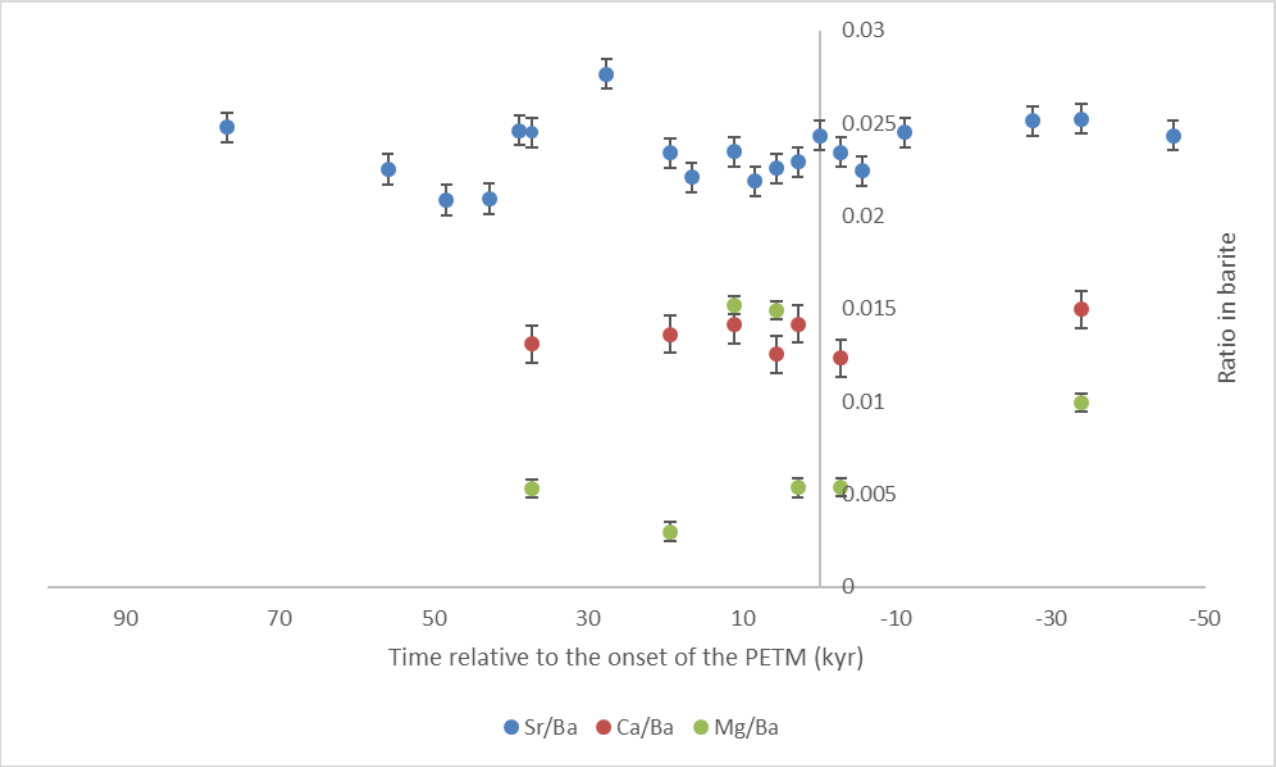

Figure 11: Element ratios as recorded in barite. The error bars indicate 1sd of individual measurements.

3.2 Sr isotope ratios

The offset of stable Sr isotopes between seawater and barite is 0.53‰ (Griffith et al., 2018). This offset was not found to be affected by local environmental conditions such as temperature. Barite records seawater radiogenic Sr isotopes, and the geological record for radiogenic Sr is well known (McArthur et al., 2012; Paytan et al., 1993). As discussed above, all presented data are preliminary and have not undergone rigorous quality control, as the method is still in progress.

The mean $^{87}Sr/^{86}Sr$ of all samples is 0.707775 (Fig. 12, upper panel), which is expected for that time (0.7077) (McArthur et al., 2012). The individual measurement error is relatively small (0.0000005). However, a long term reproducibility still needs to be established once the method is fully developed. The data appear to remain stable through the current temporal resolution, but are more scattered than data from McArthur et al., (2012). More samples will have to be analysed to improve the resolution and precision in order to assess whether any trend is distinguishable and reliable.

The mean $\delta^{88/86}Sr$ in barite of all samples is -0.26‰ (Fig. 12, lower panel), and 0.27‰ in seawater. The standard error is around 0.05‰. The expected negative excursion is not visible in the data. Rather, $\delta^{88/86}Sr$ in seawater appears to remain stable at a slightly value

lower than modern values (±0.4‰). Modern core top $\delta^{88/86}Sr$ in barite is ~-0.148‰, higher than ratios measured in our PETM samples (Paytan et al., submitted). A lower $\delta^{88/86}Sr$ in both barite and seawater is expected during the PETM, so these values seem to match that expectation, despite there not being a visible excursion. More samples will have to be analysed to increase the resolution and assess if an excursion occurred, this will be done once the TIMS method is fully developed.

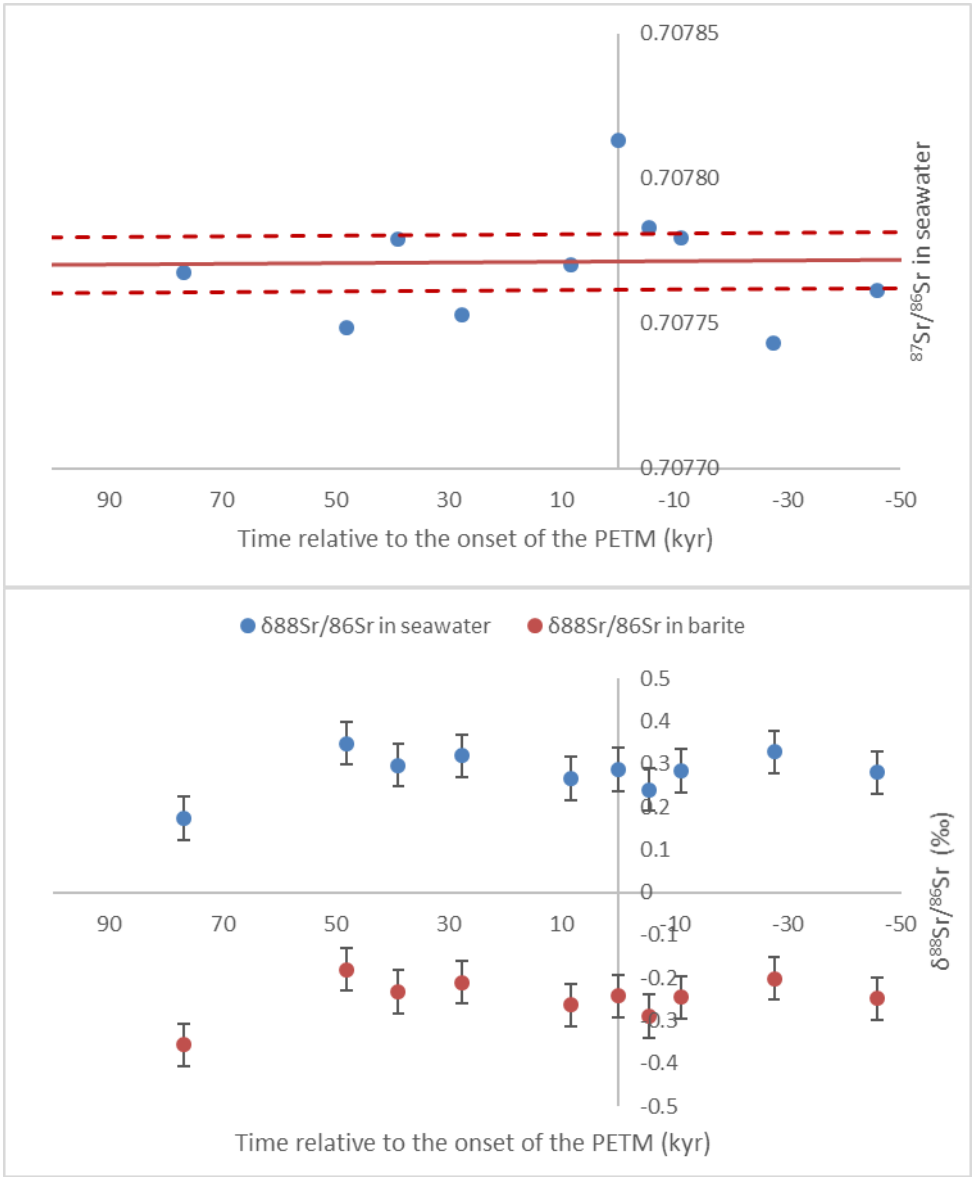

Figure 12: Preliminary Sr isotope ratio data in barite. Points indicate barite samples from this study. Red lines in upper panel are data from McArthur et al., (2012). Error bars indicate 2sd of individual measurements, this is 0.05‰ for $\delta^{88/86}Sr$ and 0.0000005 for $^{87}Sr/^{86}Sr$. This data is preliminary, and improvements in the accuracy and precision of the measurements are required.

4. Discussion

4.1 Changes in stable and radiogenic Sr

Changes in stable Sr in seawater can be interpreted as changes in carbonate deposition (Krabbenhöft et al., 2010). During the PETM, changes in carbonate deposition likely occurred in pelagic, rather than shelf, carbonates, as pelagic carbonates are the most sensitive to changes in the CCD. Increasing stable Sr isotope values indicate increasing carbonate deposition, which removes ^{86}Sr from the seawater and therefore increases stable Sr isotope ratios in seawater and consequently in barite. Decreasing stable Sr isotope values indicate decreasing carbonate deposition, or dissolution of carbonates. This either releases ^{86}Sr to the seawater or takes it up at a lower rate, decreasing the stable Sr isotope ratio of seawater.

The preliminary data produced so far do not indicate a significant negative stable Sr ratio excursion over the first 70 kyrs of the PETM (Fig. 11, lower panel). However, the mean $\delta^{88/86}Sr$ in seawater (0.27‰) is lower than that measured 100 Ma prior (0.4‰) by Vollstaedt et al., (2014). No published data is available for the Paleocene, so there is no data closer to the PETM to compare our data to. These preliminary data suggest that there was no significant effect on the Sr budget caused by carbonate dissolution. This lack of signal could indicate that not a lot of carbonate dissolved, but it is well established that carbonate dissolved during the PETM. An alternative explanation is that Sr concentrations in seawater were significantly higher than estimated, damping the input of Sr from carbonate dissolution.

Changes in radiogenic Sr reflect changes in weathering (Veizer, 1989). Decreasing values indicate increased basalt weathering or hydrothermal activity, and increasing values indicate granite weathering. This is due to differences in radiogenic Sr ratios of different lithologies. The radiogenic Sr ratio of seawater ~50 Ma was approximately 0.70777±0.0001 (McArthur et al., 2012), but it is possible that there were some fluctuations due to changes in weathering as a result of the environmental changes during and following the PETM event. Hydrothermal Sr inputs are assumed to not have changed over the PETM timescale. Preliminary $^{87/86}Sr$ values acquired from barites appear to be close to values from McArthur et al., (2012). The good agreement between our values and the established seawater curve indicate that the measurements are accurate and the samples are not significantly contaminated with modern Sr. However, the $^{87/86}Sr$ in barite data is more scattered than ideally the case. Future measurements and method development are required to assess the accuracy and improve the precision of these measurements.

4.2 Quantifying carbonate dissolution throughout the PETM

Quantification of the amount of carbonate that dissolved during the PETM can be done based on these data and the approach used for the initial estimate in Section 1.2, with additional assumptions made. Two major assumptions are that (1) the excursion occurred earlier than our data resolution, (2) the excursion is from 0.4‰ (measured by Vollstaedt et al., (2014) 75 Ma before the PETM) to 0.27‰ (measured in our data). Equation 3 can be rewritten for carbonate dissolution as such:

$$mol\ Sr_{carb\ dissolution\ input} = \frac{mol\ Sr_{initial\ sw} \cdot (\frac{\delta 88Sr}{86Sr}_{initial\ sw} - \frac{88}{86}Sr_{sw\ after\ dissolution})}{\frac{88}{86}Sr_{sw\ after\ dissolution} - \frac{\delta 88Sr}{86Sr}_{carb}} =$$

$$= \frac{1.22e17 \cdot 0.4 - 1.22e17 \cdot 0.27}{0.27 - 0.15} = 1.3e17\ mol\ Sr$$

This amounts to the dissolution of $7.5 \cdot 10^{17}$ moles of pelagic carbonate, or $4.5 \cdot 10^{19}$ g of pelagic carbonates, given a molar weight of 60.009 g/mol. Assuming that carbonate dissolved in a 1:1 ratio with carbon dioxide dissolving into the ocean (Fig. 2), this means that 9019 Pg of carbon were taken up by the ocean, given a molar weight of 12.01 g/mol for carbon. This is mostly near to or within the range of estimates of published studies (McInerney & Wing, 2011; Penman et al., 2014; Ridgwell, 2007).

5. Conclusion

Preliminary data suggest that $\delta^{88/86}$Sr in seawater was 0.13‰ lower (0.27‰) during the PETM compared to 75 Ma before the PETM (0.4‰). No excursion was apparent in the data, and there is no adjacent published data to compare these values to. Since it is unlikely that no carbonate dissolution occurred, there are two options to explain this. First, the resolution of the data might not be sufficient to capture the excursion. Second, the data may be explained by seawater Sr concentrations that were significantly higher than they are today, which would dampen the signal of Sr released through carbonate dissolution. Increasing the resolution of datapoints is a necessity for a definite conclusion, and a reconstruction of seawater Sr concentrations would provide helpful constraints.

To improve this dataset with high precision measurements, the method for TIMS analysis of Sr in barite must be further improved. This is not a trivial bit of method development and will take time. A major improvement would be the establishment of a standard that can function as an external barite standard. Currently SRM987 is used as an internal standard, and JCP and NASS-6 are used as external standards. However, neither of the latter is a barite matrix. Ideally, the external standard would be the same matrix as the samples so that any matrix effect on the measurements would be captured. As method development continues in this lab group, the long-term reproducibility and precision of TIMS measurements will be established and followed with additional analyses of PETM barite samples. The latter is key to quantifying the changes in the Sr cycle during the PETM and characterizing carbonate dissolution using Sr isotopes.

It is expected that a negative excursion will be visible, and from that excursion an estimated amount of carbonate dissolution can be calculated. If no negative excursion is visible, it will suggest that the precision of the measurement has to be further improved to see smaller differences, or that the assumed pre-PETM values (e.g. Sr seawater concentration or stable Sr ratios in carbonates) that are used in the calculation in Section 1.2 need to be revisited to figure out how much carbonate can dissolve without significantly affecting the stable Sr ratio of seawater.

This project is complex, requires more work, and has not yet managed to answer the research question. However, it has uncovered analytical challenges that particularly need our attention and provides a foundation for future work.

Acknowledgements

I would like to thank the Olaf Schuilingfonds of the Utrecht University Fund for their contribution that made this research project possible. I would like to thank Michael Tätzel and Maddie Wood for their contributions to the project.

Bibliography

Allègre, C. J., Louvat, P., Gaillardet, J., Meynadier, L., Rad, S., & Capmas, F. (2010). The fundamental role of island arc weathering in the oceanic Sr isotope budget. *Earth and Planetary Science Letters*, *292*(1–2), 51–56. https://doi.org/10.1016/j.epsl.2010.01.019

Averyt, K. B., Paytan, A., & Li, G. (2003). A precise, high-throughput method for determining Sr/Ca, Sr/Ba, and Ca/Ba ratios in marine barite. *Geochemistry, Geophysics, Geosystems*, *4*(4). https://doi.org/10.1029/2002GC000467

Böhm, F., Eisenhauer, A., Tang, J., Dietzel, M., Krabbenhöft, A., Kisakürek, B., & Horn, C. (2012). Strontium isotope fractionation of planktic foraminifera and inorganic calcite. *Geochimica et Cosmochimica Acta*, *93*, 300–314. https://doi.org/10.1016/j.gca.2012.04.038

Cuker, B., & Bugyi, G. (2016). Fundamentals of water and natural waters. In *Impact of Water Pollution on Human Health and Environmental Sustainability* (p. 28). IGI Global. https://doi.org/10.4018/978-1-4666-9559-7.ch001

Elderfield, H., & Gieskes, J. M. (1982). Sr isotopes in interstitial waters of marine sediments from Deep Sea Drilling Project cores. *Nature*, *300*(5892), 493–497. https://doi.org/10.1038/300493a0

Emerson, R. S., & Hedges, J. I. (2008). *Chemical Oceanography and the Marine Carbon Cycle*. Cambridge University Press.

Frank, M. (2002). Radiogenic isotopes: Tracers of past ocean circulation and erosional input. *Reviews of Geophysics*, *40*(1), 1001. https://doi.org/10.1029/2000RG000094

Griffith, E. M., Paytan, A., Wortmann, U. G., Eisenhauer, A., & Scher, H. D. (2018). Combining metal and nonmetal isotopic measurements in barite to identify mode of formation. https://doi.org/10.1016/j.chemgeo.2018.09.031

Hess, J., Bender, M. L., & Schilling, J. G. (1986). Evolution of the Ratio of Strontium-87 to Strontium-86 in Seawater from Cretaceous to Present. *Science*, *231*(4741), 979–984. https://doi.org/10.1126/science.231.4741.979

Krabbenhöft, A., Eisenhauer, A., Böhm, F., Vollstaedt, H., Fietzke, J., Liebetrau, V., … Wallmann, K. (2010). Constraining the marine strontium budget with natural strontium isotope fractionations (87Sr/86Sr∗, δ88/86Sr) of carbonates, hydrothermal solutions and river waters. *Geochimica et Cosmochimica Acta*, *74*(14), 4097–4109. https://doi.org/10.1016/J.GCA.2010.04.009

Krabbenhöft, Andre, Fietzke, J., Eisenhauer, A., Liebetrau, V., Böhm, F., & Vollstaedt, H. (2009). Determination of radiogenic and stable strontium isotope ratios (87Sr/86Sr; δ88/86Sr) by thermal ionization mass spectrometry applying an 87Sr/84Sr double spike. *Journal of Analytical Atomic Spectrometry*, *24*(9), 1267. https://doi.org/10.1039/b906292k

McArthur, J. M., Howarth, R. J., & Shields-Zhou, G. A. (2012). Strontium isotope stratigraphy. https://doi.org/10.1016/B978-0-444-59425-9.00007-X

McInerney, F. A., & Wing, S. L. (2011). The Paleocene-Eocene Thermal Maximum: A Perturbation of Carbon Cycle, Climate, and Biosphere with Implications for the Future.

Annual Review of Earth and Planetary Sciences, *39*(1), 489–516. https://doi.org/10.1146/annurev-earth-040610-133431

Mearon, S., Paytan, A., & Bralower, T. J. (2003). Cretaceous strontium isotope stratigraphy using marine barite. *Geology*, *31*(1), 15. https://doi.org/10.1130/0091-7613(2003)031<0015:CSISUM>2.0.CO;2

Mokadem, F., Parkinson, I. J., Hathorne, E. C., Anand, P., Allen, J. T., & Burton, K. W. (2015). High-precision radiogenic strontium isotope measurements of the modern and glacial ocean: Limits on glacial-interglacial variations in continental weathering. *Earth and Planetary Science Letters*, *415*, 111–120. https://doi.org/10.1016/j.epsl.2015.01.036

Neymark, L. A., Premo, W. R., Mel'Nikov, N. N., & Emsbo, P. (2014). Precise determination of δ^{88}Sr in rocks, minerals, and waters by double-spike TIMS: A powerful tool in the study of geological, hydrological and biological processes. *Journal of Analytical Atomic Spectrometry*, *29*(1), 65–75. https://doi.org/10.1039/c3ja50310k

Ohno, T., & Hirata, T. (2007). Simultaneous determination of mass-dependent isotopic fractionation and radiogenic isotope variation of strontium in geochemical samples by multiple collector-ICP-mass spectrometry. *Analytical Sciences*, *23*(11), 1275–1280. https://doi.org/10.2116/analsci.23.1275

Palmer, M. R., & Elderfield, H. (1985). Sr isotope composition of sea water over the past 75 Myr. *Nature*, *314*(6011), 526–528. https://doi.org/10.1038/314526a0

Paytan, A., Averyt, K., Faul, K., Gray, E., & Thomas, E. (2007). Barite accumulation, ocean productivity, and Sr/Ba in barite across the Paleocene-Eocene Thermal Maximum. *Geology*, *35*(12), 1139–1142. https://doi.org/10.1130/G24162A.1

Paytan, A., Griffith, E. M., & Fisher, A. (n.d.). A 35 Myr Record of Seawater Stable Sr Isotopes from Marine Barite and its Use for Construing Changes in Seawater Sr concentrations and Carbonate Deposition History.

Paytan, A., Kastner, M., Martin, E. E., Macdougall, J. D., & Herbert, T. (1993). Marine barite as a monitor of seawater strontium isotope composition. *Nature*, *366*(6454), 445–449. https://doi.org/10.1038/366445a0

Paytan, A., Mearon, S., Cobb, K., & Kastner, M. (2002). Origin of marine barite deposits: Sr and S isotope characterization. *Geology*, *30*(8), 747. https://doi.org/10.1130/0091-7613(2002)030<0747:OOMBDS>2.0.CO;2

Pearce, C. R., Parkinson, I. J., Gaillardet, J., Charlier, B. L. A., Mokadem, F., & Burton, K. W. (2015). Reassessing the stable (δ88/86Sr) and radiogenic (87Sr/86Sr) strontium isotopic composition of marine inputs. *Geochimica et Cosmochimica Acta*. https://doi.org/10.1016/j.gca.2015.02.029

Penman, D. E., Hönisch, B., Zeebe, R. E., Thomas, E., & Zachos, J. C. (2014). Rapid and sustained surface ocean acidification during the Paleocene-Eocene Thermal Maximum. *Paleoceanography*, *29*(5), 357–369. https://doi.org/10.1002/2014PA002621

Ridgwell, A. (2007). Interpreting transient carbonate compensation depth changes by marine sediment core modeling. https://doi.org/10.1029/2006PA001372

Röhl, U., Westerhold, T., Bralower, T. J., & Zachos, J. C. (2007). On the duration of the Paleocene-Eocene thermal maximum (PETM). *Geochemistry, Geophysics, Geosystems*, *8*(12), n/a-n/a. https://doi.org/10.1029/2007GC001784

Scher, H. D., Griffith, E. M., & Buckley, W. P. (2014). Accuracy and precision of 88 Sr/ 86 Sr and 87 Sr/ 86 Sr measurements by MC-ICPMS compromised by high barium concentrations. *AGU Publications*. https://doi.org/10.1002/2013GC005134

Stoll, H. M., & Schrag, D. P. (1998). Effects of Quaternary sea level cycles on strontium in

seawater. *Geochimica et Cosmochimica Acta*, *62*(7), 1107–1118. https://doi.org/10.1016/S0016-7037(98)00042-8

Teng, F. (2017). Magnesium Isotope Geochemistry. *Reviews in Mineralogy and Geochemistry*, *82*(1), 219–287. https://doi.org/10.2138/rmg.2017.82.7

Vance, D., Teagle, D. A. H., & Foster, G. L. (2009). Variable Quaternary chemical weathering fluxes and imbalances in marine geochemical budgets. *Nature*, *458*(7237), 493–496. https://doi.org/10.1038/nature07828

Veizer, J. (1989). *Strontium isotopes in seawater through time*. *Ann. Rev. Earth Planet. Sci* (Vol. 17). Retrieved from www.annualreviews.org

Vollstaedt, H., Eisenhauer, A., Wallmann, K., Böhm, F., Fietzke, J., Liebetrau, V., … Veizer, J. (2014). The Phanerozoic δ88/86Sr record of seawater: New constraints on past changes in oceanic carbonate fluxes. *Geochimica et Cosmochimica Acta*, *128*, 249–265. https://doi.org/10.1016/J.GCA.2013.10.006

Yao, W., Paytan, A., & Wortmann, U. G. (2018). Large-scale ocean deoxygenation during the Paleocene-Eocene Thermal Maximum. *Science*. https://doi.org/10.1126/science.aar8658

Zachos, J. C., Röhl, U., Schellenberg, S. A., Sluijs, A., Hodell, D. A., Kelly, D. C., … Kroon, D. (2005). Rapid acidification of the ocean during the Paleocene-Eocene thermal maximum. *Science (New York, N.Y.)*, *308*(5728), 1611–1615. https://doi.org/10.1126/science.1109004

Zeebe, R. E., Zachos, J. C., & Dickens, G. R. (2009). Carbon dioxide forcing alone insufficient to explain Palaeocene--Eocene Thermal Maximum warming. https://doi.org/10.1038/NGEO578